Endoplasmic Reticulum Stress and the Lysosomal Pathway Play Crucial Roles in the Progression of βB2-Crystallin Mutation-Induced Congenital Cataracts in Mice

Wei Xiao, Weimin Yang, Xinyu Zhang, Xiaoqian Deng, and Xiaoyun Chen

State Key Laboratory of Ophthalmology, Zhongshan Ophthalmic Center, Sun Yat-Sen University, Guangdong Provincial Key Laboratory of Ophthalmology and Visual Science, Guangzhou, China

Correspondence: Xiaoyun Chen and Wei Xiao, State Key Laboratory of Ophthalmology, Zhongshan Ophthalmic Center, Sun Yat-Sen University, Guangzhou 510060, China;
chenxiaoyun@gzzoc.com and xiaowei@gzzoc.com.

Received: January 8, 2023
Accepted: April 5, 2023
Published: April 27, 2023

Citation: Xiao W, Yang W, Zhang X, Deng X, Chen X. Endoplasmic reticulum stress and the lysosomal pathway play crucial roles in the progression of βB2-crystallin mutation-induced congenital cataracts in mice. *Invest Ophthalmol Vis Sci.* 2023;64(4):34. https://doi.org/10.1167/iovs.64.4.34

Purpose. Congenital cataract is a major cause of visual impairment and childhood blindness; however, its underlying mechanism remains unclear. Here, we aimed to identify the roles of endoplasmic reticulum stress (ERS), lysosomal pathway, and lens capsule fibrosis during the progression of βB2-crystallin mutation-induced congenital cataract in mice.

Methods. BetaB2-W151C knock-in mice were generated using the CRISPR/Cas9 system. Lens opacity was assessed with a slit-lamp biomicroscopy and dissecting microscope. Transcriptional profiles of the lenses in W151C mutant and wild-type (WT) control mice were detected at 3 months of age. Immunofluorescence of lens anterior capsule was photographed with a confocal microscope. Real-time PCR and immunoblot were used to detect gene mRNA and protein expressions, respectively.

Results. BetaB2-W151C knock-in mice developed progressive bilateral congenital cataracts. At 2 to 3 months of age, lens opacity rapidly progressed to complete cataracts. Additionally, multilayered LEC plaques developed beneath the lens anterior capsule in homozygous mice at 3 months of age, and severe fibrosis was observed in the whole lens capsule at 9 months of age. Microarray analysis of whole genome transcriptomics and the validation results of real-time PCR revealed that genes of ERS, the lysosomal pathway, apoptosis, and cell migration and fibrosis were significantly upregulated in βB2-W151C mutant mice during the accelerated development of cataract. Moreover, the syntheses of various crystallins stagnated in βB2-W151C mutant mice.

Conclusions. ERS, the lysosomal pathway, apoptosis, and fibrosis all contributed to the accelerated development of congenital cataract. The inhibition of ERS and lysosomal cathepsins may be promising therapeutic strategies for congenital cataract.

Keywords: congenital cataract, endoplasmic reticulum stress (ERS), lysosome, apoptosis, fibrosis

Congenital cataract is a major cause of visual impairment and blindness in children. The pathogenic causes are complex; approximately one third of cases are hereditary, and more than half are caused by mutations in crystallin genes.[1] Beta-crystallins are the most abundant water-soluble proteins in the lens, and most of them are expressed in lens cortical fiber cells. They play key roles in the development and maintenance of lens transparency. BetaB2 is the major β-crystallin and is also the most thermally stable and soluble of all β-crystallins.[2,3] Previous studies have reported that heterogeneous and homogeneous crystallin interactions exist among α, β, and γ-crystallins.[4,5] Mutations in βB2-crystallin not only change its tertiary structure but also alter protein-protein interactions, resulting in unstable protein with more hydrophobic surfaces exposed that precipitate from solution and facilitate additional protein precipitation.[4–6] In our previous study, we identified a missense mutation in βB2-crystallin (W151C) in a Chinese family affected with congenital membranous cataracts.[7] However, in addition to the decrease of crystallin solubility, whether there are other underlying molecular mechanisms involved in cataract development is currently unclear.

Increasing evidence has confirmed that endoplasmic reticulum stress (ERS) plays an important role in a variety of protein aggregation diseases, such as Alzheimer's disease, Parkinson's disease, retinal degeneration, and cataract.[8–11] ERS can be triggered by the accumulation of unfolded proteins in the endoplasmic reticulum (ER) induced by oxidative stress, calcium metabolism disorders, and mutations in coding genes. When ERS is triggered, cells activate a series of defense mechanisms known as the unfolded protein response (UPR), which can reduce the accumulation of abnormal proteins and restore ER homeostasis by reducing protein synthesis, enhancing protein folding, and accelerating the clearance of unfolded or misfolded proteins.[12] In congenital cataract, it has been reported that mutations

in connexin 50, βA3/A1-crystallin, and αB-crystallin cause abnormal accumulation of mutant proteins in the ER of the mouse lens, which further activates the UPR and induces apoptosis in lens fiber cells.[13–16] In addition, it was also found that the accumulation of abnormal collagen IV initiated the UPR in Col4a1 mutant mouse cataract model, and reduced the synthesis of β and γ-crystallin, destroyed lens fiber differentiation, and induced cell apoptosis.[17] Nevertheless, the role of ERS in βB2-crystallin mutant-induced congenital cataract is unknown.

Lysosomes are another key degradation compartment for abnormal organelles and proteins in cells. They are critical in the quality control of organelles and proteins and cellular homeostasis. However, lysosomes and lysosomal cathepsins have been reported to have dual roles in cell death. Although degrading heterophagic and autophagic materials, cathepsins initiate apoptosis through the cleavage of Bid and the degradation of the antiapoptotic Bcl-2 homologs.[18] Previous studies have reported that autophagy is impaired and that P62 accumulates in cataracts caused by mutations in *CHMP4B*, *FYCO1*, *RRAGA*, *TDRD7*, αB-crystalline, and βA3/A1-crystallin.[19–24] However, the downstream effects and lysosomal pathway have not been examined, especially the roles of lysosomal cathepsins in the progression of congenital cataract.

In this study, we generated knock-in mice expressing βB2-crystallin protein containing the W151C mutation, which mimics a human mutation, to explore the pathogenesis and molecular mechanisms of hereditary cataract.

Methods

Generation of the βB2-W151C Knock-In Mouse Model

BetaB2-W151C knock-in mice expressing a G to C point mutation in codon 151 of the mouse βB2-crystallin gene *Crybb2*, which results in the substitution of Tryptophan 151 with Cysteine (W151C), were generated using the CRISPR/Cas9 system by Shanghai Biomodel Organisms Science and Technology Development Co., Ltd. (Shanghai, China). The mice were generated by gene insertion mediated by CRISPR/Cas9 in C57BL/6J zygotes, which modified *Crybb2* such that exon 7 contained the W151C mutation in one allele, whereas the second copy of the gene was wild-type (WT). The G to C mutation was verified by sequencing the genomic DNA when F0 generation mice were 14 days old. Chimeric founders were mated with WT C57BL6 mice. Heterozygous (W151C+/−) offspring were subsequently mated with each other to yield homozygous mice (W151C+/+), which contained two copies of the mutant gene.

The mice were maintained at Zhongshan Ophthalmic Center at Sun Yat-Sen University (Guangzhou, China). All protocols and animal procedures were approved by the Animal Use and Care Committee of Zhongshan Ophthalmic Center and conformed to the ARVO Statement for the Use of Animals in Ophthalmic and Vision Research. WT littermates were used as controls.

Assessment of Lens Opacity With Slit-Lamp Biomicroscopy

Knock-in and WT mice were anesthetized with an intraperitoneal injection of pentobarbital sodium (70 mg/kg). Pupils were dilated with a mixture of 0.5% phenylephrine hydrochloride and 0.5% tropicamide (Santen, Suzhou, Japan). Approximately 15 minutes later, each mouse was held gently by the scruff of the neck and positioned directly facing the slit lamp. Both eyes were then examined and photographed with a slit lamp biomicroscopy.

Assessment of Lens Opacity With a Dissecting Microscope and Morphometric Analysis

The eyes of knock-in and WT mice were enucleated and maintained in phosphate-buffered saline (PBS). The length between the central corneal epithelium and the central point of the optic nerve head was measured as eye size with a microscale under the dissecting microscope (Carl Zeiss, Overkochen, Germany). Then, the whole lenses were carefully isolated and photographed. Lens diameter was also measured as lens size.

Histological Analysis

For histological analysis, the eyes of knock-in and WT mice were removed and fixed in 4% paraformaldehyde (PFA) overnight. After dehydration and clarification, they were embedded in paraffin and sectioned serially at 4 µm thickness via the pupil-optic nerve plane, then stained with hematoxylin and eosin. The sections were evaluated by a fluorescence microscope (Carl Zeiss, Overkochen, Germany).

Immunofluorescence and Laser Confocal Microscopy

The immunofluorescences of whole mount lens anterior capsules of knock-in and WT mice were performed according to our previously described method.[25]

Whole Genome Transcriptome Analysis of Lenses and Bioinformatics Analysis

Preparation of lens RNA samples of WT and homozygous knock-in mice at 3 months of age and the Whole mouse genome oligo microarray were performed by KangCheng Bio Co. Ltd. (Shanghai, China). Four lenses from two mice of the same genotype were combined into one sample ($n = 3$). Principal component analysis (PCA) was conducted using the factoextra package (version 1.0.7). The R package limma (version 3.52.2) was applied to analyze the gene expression of the microarray data.[26] Differentially expressed genes (DEGs) were defined as those with log2 fold change (log2FC) ≥ 1 or ≤ -1 and adjusted P values < 0.05 between the 2 group samples. A volcano plot was used to visualize DEGs, and genes of interest were labeled. Gene set enrichment analysis (GSEA), Gene Ontology (GO), and Kyoto Encyclopedia of Genes and Genomes (KEGG) pathway analyses were performed using the R package clusterProfiler (version 4.4.4).[27] Heatmaps were created with the R package pheatmap (version 2.6.2). The data are publicly available in the Gene Expression Omnibus (GEO) repository (GSE 225548), and the R script used for bioinformatic analysis is attached as Supplementary File S1.

Real-Time Quantitative PCR Analysis for Gene Expression

The lenses of WT and knock-in mice were isolated on ice and stored in TRIzol reagent at −80°C for no more than 1 month.

Investigative Ophthalmology & Visual Science

Total RNA was extracted on ice according to the manufacturer's protocol. Four lenses from two mice of the same genotype were combined into one sample. The cDNAs synthesis was performed using a PrimeScript RT Master Mix kit (Takara, Siga, Japan) following the manufacturer's protocol. Briefly, 20 µL of the reaction mixture was added to respective Eppendorf tubes: 4 µL of the PrimeScript RT Master mix (5x), 1000 ng of total RNA, and RNase-free water to 20 µL. The samples were then incubated at 37°C for 15 minutes and at 85°C for 5 seconds for enzyme inactivation. Real-time PCRs were performed using the SYBR PrimeScript RT-PCR kit (Takara, Siga, Japan) in 20 µL reactions with an ABI Prism 7000 sequence detection system (Applied Biosystems, Foster City, CA, USA) according to the Minimum Information for Publication of Quantitative RT PCR Experiments (MIQE) guidelines.[28] All the primers were designed to cross introns. Briefly, 10 µL of SYBR Premix Ex Taq (2x), 0.4 µL of 20 µmol/L forward and reverse primers, 0.4 µL of ROX reference dye (50x), 2 µL of the cDNA template, and 6.8 µL of nuclease-free water were added to each well of a 96-well PCR plate, in duplicate. The standard procedure for two-step PCR amplification was performed: pre-denaturation (95°C for 30 seconds), PCR cycling (40 cycles) for denaturation (95°C for 5 seconds), and annealing (60°C for 30 seconds). Melt curve analysis was used to ensure single PCR products were produced. Glyceraldehyde 3-phosphate dehydrogenase (GAPDH) was used as an internal control to normalize relative fold expression and relative expression of mRNA was calculated using the established $2^{-\Delta\Delta CT}$ method. A quantification cycle (Cq) value ≥34 was considered an outlier. The experiments were repeated independently three or more times. The primers used in this study are listed in Supplementary Table S1.

Immunoblot Analysis

Lens protein expressions were detected by immunoblot performed according to our previously described method.[25] The primary antibodies against β-actin, Perk, p-Perk, Eif2a, p-Eif2a, Atf4, Ire-1a, horse anti-mouse, and goat anti-rabbit horseradish peroxidase (HRP) conjugates secondary antibodies were obtained from Cell Signaling Technology (Danvers, MA, USA). Antibodies against α-crystallin, β-crystallin, and γ-crystallin were obtained from Abcam (Cambridge, UK).

Statistical Analysis

Results presented in the figures are representative of three or more different repetitions. All data are presented as mean ± standard error of the mean (SEM). The data were analyzed by using two-tailed Student *t*-test. A value of $P < 0.05$ was considered statistically significant.

Results

BetaB2-W151C Knock-In Mice Exhibit Progressive Bilateral Congenital Cataracts

In humans, the βB2-crystallin W151C mutation results in a progressive bilateral congenital cataract.[7] BetaB2-W151C heterozygous mice that mimic the heterozygosity of human patients have one mutant allele and one WT allele. To investigate the phenotype of the βB2-W151C mutant during the postnatal period, we observed the ocular structure with a dissecting microscope and slit lamp microscopy. The external morphologies of the eyes and the dissected lenses from βB2-W151C knock-in mice did not appear different from WT mice at birth. As shown in Figure 1A, starting at 18 days of age, punctate lens opacities located at the peripheral cortex were observed in all homozygous mice, and the same change began to appear in heterozygous mice at 21 days of age. Punctate peripheral lens opacities extended gradually and became denser with aging. At approximately 1.5 months, Y-suture opaque appeared in both heterozygous and homozygous mice. At 2 to 3 months of age, cataracts progressed rapidly. The whole lens became opaque by 2.5 months of age in all homozygous mice and at 3 months in heterozygous mice. No cataracts were observed in WT mice before 18 months of age (see Fig. 1A). In mice older than 6 months, the lens cortex started to liquefy, and the lenses shrank gradually in homozygous mice. Additionally, the leaky lens cortex could induce uveitis, resulting in the synechia of the iris (Fig. 1B).

There was no significant change in lens growth among WT, heterozygous, and homozygous mice after birth. However, lens diameter started to decrease from 6 months of age in homozygous mice and at 9 months of age in heterozygous mice due to hydrolysis of the lens cortex. Moreover, no significant difference in eyeball size was observed between knock-in and WT mice (Fig. 1C).

Histological Changes in the Lenses of βB2-W151C Knock-In Mice

Representative examples of lens histology for βB2-W151C knock-in mice compared with WT lenses are shown in Figure 2. Fiber cell migration and elongation patterns were found to be defective at the equatorial and anterior regions in lenses from βB2-W151C knock-in mice at 3 months of age (see Fig. 2A). Additionally, lenses developed remarkable multilayered LEC plaques beneath the lens anterior capsule in homozygous mice at 3 months of age, and those were also found in heterozygous mice at 9 months of age. Lens anterior capsule whole-mount staining also showed that multilayered LEC plaques began to appear in homozygous lenses at 3 months of age, whereas the anterior capsules from heterozygous mice still retained a single layer of epithelium. The severity of plaques beneath the lens anterior capsule developed gradually, and extremely severe fibrosis was observed in the whole lens capsules of homozygous mice at 9 months of age (see Figs. 2A, 2B). These findings indicated fibrosis of the lens capsule and destruction of the structural integrity of the lens epithelium and capsule, which may contribute to liquidation of the lens cortex in the late stage of congenital cataracts.

Transcriptional Profiling of the Lenses of W151C Mutant Mice Compared With Those of WT Mice

To evaluate the impact of the βB2-W151 mutation on the expression profiles of the lens, the lenses of W151C+/+ mutant and WT control mice were isolated, and their transcriptional profiles were detected at the age of 3 months, when the lens opacity developed into complete cataracts. Transcriptome analysis revealed distinct differences in the expression profiles in the lenses of W151C+/+ mutant mice compared with WT mice (Fig. 3A). DEGs were visualized in the volcano plot, and the top five expressed genes related to biological processes of interest were labeled (Fig. 3B). GSEA showed that the highly expressed genes

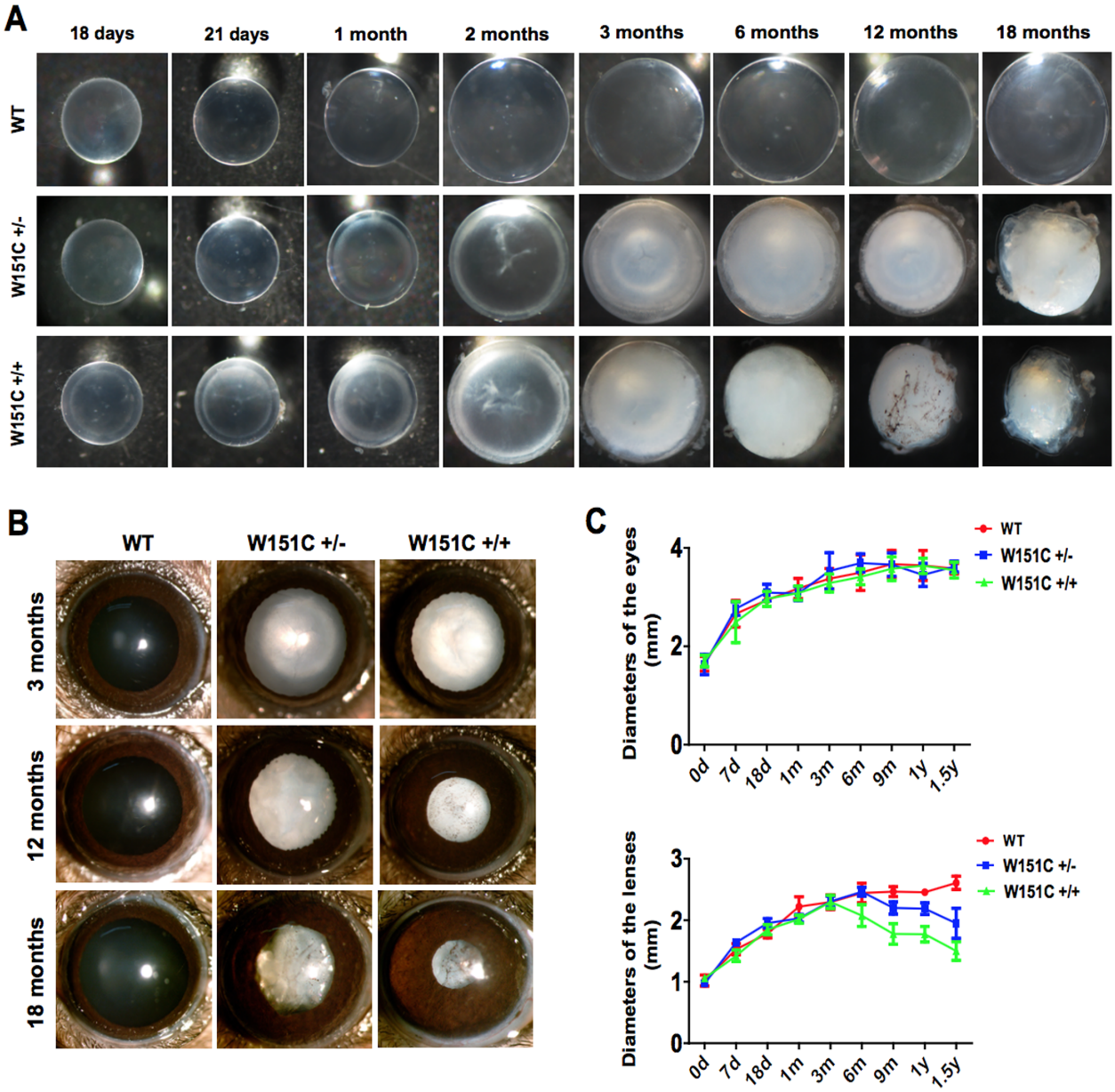

Figure 1. BetaB2-W151C knock-in mice exhibit progressive bilateral congenital cataracts. (**A**) The lenses of heterozygous, homozygous, and WT mice were isolated at different ages and photographed with a dissecting microscope ($n = 8$ lenses per group). (**B**) The eyes of WT, heterozygous, and homozygous mice were examined and photographed with a slit lamp after dilation of the pupils ($n = 8$ eyes per group). (**C**) The diameters of the eyes and the lens of heterozygous, homozygous, and WT mice were measured with a microscale under a dissecting microscope ($n = 8$ eyes or lenses per group).

in W151C+/+ mutant lenses contributed significantly to biological processes such as the extrinsic apoptotic signaling pathway, intrinsic apoptotic signaling pathway in response to ERS, lysosome pathway, regulation of cell migration, and fibroblast proliferation (Fig. 3C). These analyses suggested that ERS, the lysosome pathway, apoptosis, and epithelial mesenchymal transition (EMT) may be involved in the rapid development of congenital cataracts.

ERS is Triggered in the Rapid Development of Congenital Cataract Induced by the βB2-W151C Mutant Mice

Previous studies have confirmed that the accumulation of unfolded mutated abnormal proteins can disrupt ER homeostasis and trigger ERS. Our microarray analysis of whole genome transcriptomics revealed that many ERS-related genes were significantly upregulated in homozygous mice compared with WT controls at the age of 3 months (Fig. 4A). The top two upregulated genes in the W151C +/+ lens were *Trib3* (>80-fold) and *Chac1* (>20-fold), two proapoptotic components of the UPR.[29] In addition, several transcription-factor components of the UPR were also upregulated (>2-fold) in the W151C +/+ lens, including *Ddit3*, *Atf4*, *Atf3*, and *Cebpb*, along with their downstream target genes *Hspb8*, *Hsph1*, *Dnajc15*, *Dnajc9*, *Dnajc2*, and *Dnajc6*.

Afterward, we validated the transcript levels of representative ERS-related genes using real-time PCR analysis. Consistent with the microarray findings, 11 genes, including *Trib3*, *Chac1*, *Atf4*, *Atf5*, *Ddit3*, *Chop*, *Hspb8*, *Hsph1*, *Dnajc15*, and *Cebpb*, were dramatically upregulated in both

Investigative Ophthalmology & Visual Science

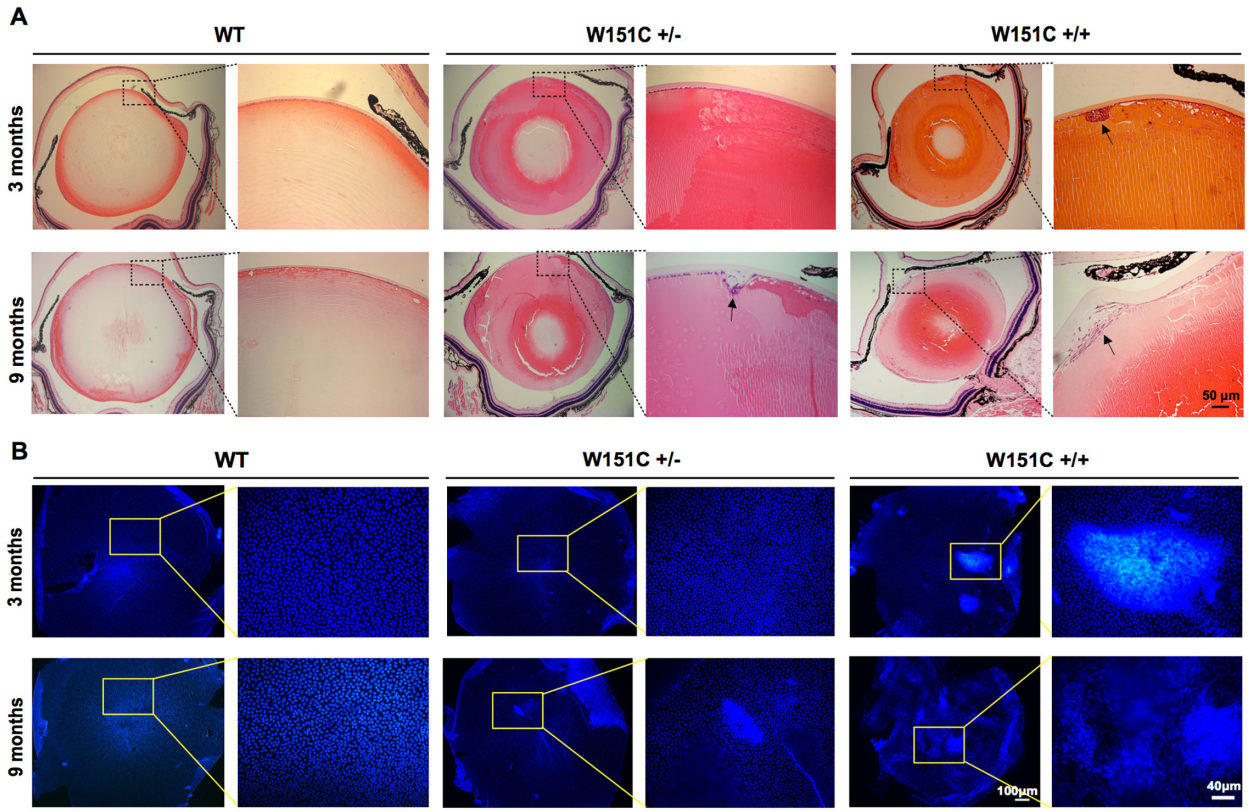

Figure 2. Morphological changes in the lenses of βB2-W151C knock-in mice. **(A)** The eyes of WT and βB2-W151C knock-in mice were analyzed by hematoxylin/eosin staining ($n = 8$ eyes per group). **(B)** Representative images of immunofluorescent DAPI staining of lens capsule whole-mounts ($n = 8$ eyes per group).

W151C homozygous and heterozygous lenses (Fig. 4B). Although *Atf3* was not significantly upregulated in the microarray data, it was increased in the real-time PCR data. In contrast, the expressions of *Dnajc2*, *Dnajc6*, and *Dnajc9* did not obviously chance in real-time PCR analysis. Furthermore, the results from Western blot also displayed that the W151C mutation significantly activated the ERS-related signaling pathways p-Perk, p-Eif2α, and Atf4, and slightly increased Ire-1 expression during the rapid progression of lens opacity. Taken together, these results indicated that ERS was triggered by the accumulation of abnormal βB2-crystallin during the rapid development of W151C mutant-induced congenital cataracts.

ERS-Mediated Stagnation of Crystallin Synthesis Plays a Critical Role During the Accelerated Development of Congenital Cataract

ERS can reduce protein synthesis via the UPR to restore ER homeostasis. Therefore, we next investigated whether the expression of crystallins was downregulated in the lens. Real-time PCR was used to detect the mRNA levels of α-, β-, and γ-crystallin genes in the lenses of W151C +/− and W151C +/+ mice at 1, 2, 3, and 9 months after birth. The results showed that the mRNA levels of *Cryba1*, *Cryba4*, *Crybb1*, *Crybb2*, *Crygb*, *Crygc*, and *Crygd* were almost stopped at the age of 3 months, and *Cryaa* and *Cryab* were also dramatically downregulated at 9 months of age (Fig. 5A). Moreover, the results of Western blot also confirmed that the synthesis of α-, β-, and γ-crystallin stagnated at 3 months (Fig. 5B). These results suggested that ERS-mediated stagnation of lens structural protein synthesis is one of the important causes of accelerated cataract development.

The Lysosomal Pathway Is Also Involved in the Rapid Progression of Congenital Cataract Induced by the βB2-W151C Mutant Mice

Lysosomes are known as intracellular "suicide bags." In particular, cathepsins play a major role in maintaining cell homeostasis by degrading abnormal organelles and proteins. Cathepsins can also be released into the cytosol and initiate the lysosomal pathway of apoptosis. Whole genome transcriptomics and GO and KEGG analyses showed that the lysosomal pathway was enriched in the W151C +/+ lens at 3 months of age (Figs. 6A, 6B). The heatmap showed that up to 45 genes related to the lysosomal pathway were significantly increased in the W151C +/+ lenses (Fig. 6C). The top five expressed genes were *Ada* (adenosine deaminase), *Ctsc* (cathepsin C), *Ctss* (cathepsin S), *Mt1* (metallothionein 1), and *Cd68* (lysosomal antigen CD68). In particular, multiple lysosomal cathepsins including cathepsin S, cathepsin B, cathepsin C, cathepsin L, and cathepsin H were dramatically elevated in the W151C +/+ lenses (see Fig. 6C). The real-time PCR results also verified that cathepsins were dramatically upregulated in both W151C homozygous and

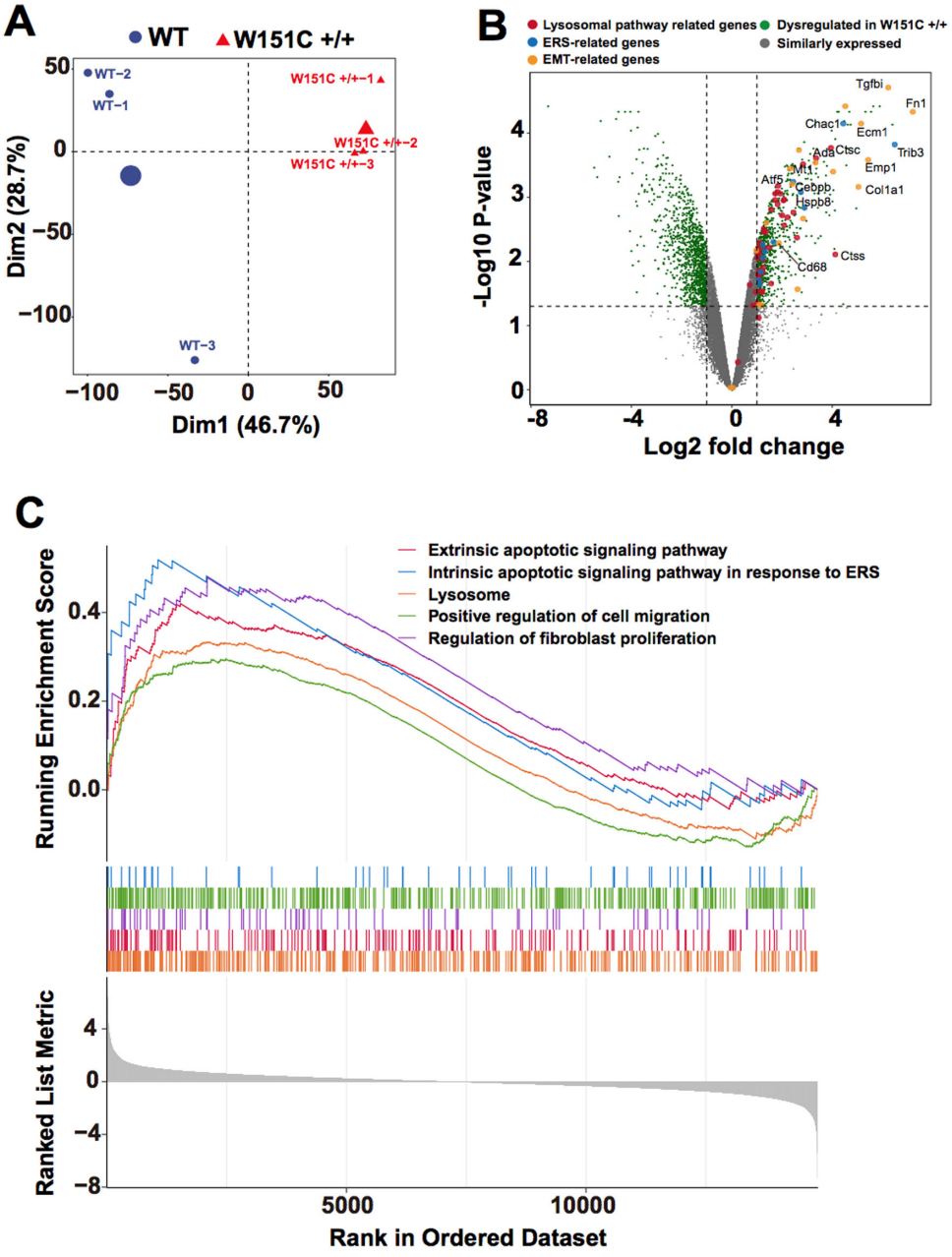

Figure 3. Transcriptional profiling of the lenses of W151C mutant mice compared to those of WT mice. Lenses of W151C +/+ mutant and WT control mice were harvested, and their transcriptional profiles were detected at the age of 3 months. Four lenses from two mice of the same genotype were combined into one sample ($n = 3$). (**A**) Principal component analysis (PCA) was conducted to reveal the expression profiles of the lenses of W151C +/+ mutant and WT mice. The larger symbol is the mean value for each group. (**B**) Differentially expressed genes (DEGs) were visualized in the volcano plot, and the top five expressed genes related to biological processes of interest were labeled. The horizontal dotted grid line is placed at the minus logarithm (base 10) of the *P* value being 1.301, corresponding to a *P* value of 0.05; the *vertical dotted lines* indicate the logarithm (base 2) of the fold change -1 and 1, indicating that the actual fold change was 0.5 and 2, respectively. (**C**) Gene set enrichment analysis (GSEA) was performed using the R package clusterProfiler to reveal the biological processes and molecular functions involved in highly expressed genes. The Running Enrichment Score indicates the magnitude to which the genes in a certain gene set are overrepresented within the entire ranked list of genes. Ranked List Metric shows the value of the ranking metric (log2-fold change) as moving down the list of ranked genes.

heterozygous lenses (Fig. 6D). In addition, KEGG analysis revealed that apoptosis-related genes were enriched in the W151C +/+ lens (see Fig. 6B). These results suggested that the lysosomal pathway, especially cathepsins, plays a major role in the rapid progression of congenital cataracts by inducing apoptosis and excessive degradation of lens proteins.

LEC EMT and Lens Capsule Fibrosis Contribute to Lens Cortex Liquefaction in the Late Stage of Congenital Cataract

The anterior lens capsule and lens epithelium serve as barriers and play vital roles in maintaining lens homeostasis and transparency. When EMT occurs in LECs, the connections

Investigative Ophthalmology & Visual Science

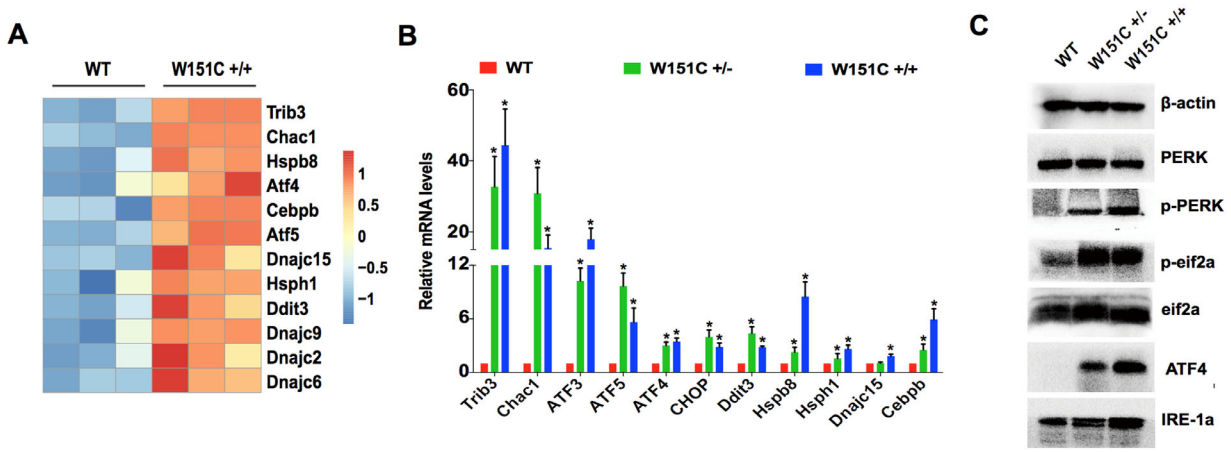

Figure 4. ERS is triggered during the rapid development of congenital cataracts induced by the βB2-W151C mutant. (**A**) Heatmap showing that ERS-related genes were dramatically upregulated in the lenses of W151C +/+ mutant mice at 3 months of age. (**B**) Real-time PCR analysis was used to validate the transcript levels of ERS-related genes in the lenses of W151C +/−, W151C +/+ and WT mice. *, $P < 0.05$ versus WT control mice. The experiments were repeated independently three or more times. (**C**) The ERS-related signaling factors p-Perk, Perk, p-Eif2α, Eif2α, Atf4, and Ire-1 were detected by Western blot analysis. The experiments were repeated independently three or more times.

between LECs are impaired, and barrier function is destroyed.[30] To investigate the molecular mechanism of the fibrosis of the lens capsule and epithelium in W151C mutant mice, we focused on the expression of cell migration, adhesion, extracellular matrix (ECM) component deposition, and EMT-related genes via whole genome transcriptomics analysis. Microarray analysis revealed that more than 20 related genes were significantly upregulated in homozygous mice compared with WT controls (Fig. 7A). Next, we validated these genes using real-time PCR analysis. Consistent with the microarray findings, 17 genes were dramatically upregulated in homozygous and heterozygous mutant mice at the age of 3 months. The top two upregulated genes in the W151C +/+ lens were *Tgfbi* (transforming growth factor β induced; 89.0-fold) and *Ecm1* (92.6-fold). In addition, several EMT markers were upregulated (>4-fold) in the W151C +/+ lens, including *FN*, *Col I*, *Col IV*, *Snail*, and *Slug* (Fig. 7B). Moreover, strong staining of the EMT markers α-SMA, Col I, vimentin, and FN could be seen in lenses that developed remarkable multilayered LEC plaques. Due to the fibrosis of the lens capsule, its barrier function was damaged, permeability was changed, the lens cortex liquefied gradually, and the lens shrank. At 9 months, the lenses became significantly smaller in homozygous mice. Taken together, these results indicated that the disruption of barrier function caused by lens epithelial cell (LEC) EMT and lens capsule fibrosis is the main cause of the gradual liquefaction of the lens cortex in the late stage of congenital cataracts.

Discussion

Congenital cataract occurs in the critical stage of visual development, when lens opacity severely affects the development of visual function in children. Surgery is the only effective way to treat congenital cataract, but there are many complications such as uveitis, glaucoma, and posterior capsule opacification, resulting in poor efficacy.[31] Therefore, there is an urgent need to understand the underlying mechanisms. In this study, we used a mouse congenital cataract model induced by the W151C mutation in βB2-crystallin to further elucidate the molecular mechanisms of congenital cataract. We found that βB2-W151C knock-in mice developed progressive bilateral congenital cataracts. At 2 to 3 months of age, cataracts progressed rapidly and developed into complete cataracts at 3 months of age. More interestingly, in addition to the decrease in protein solubility caused by the mutation,[32] ERS and ERS-mediated protein synthesis stagnation, the lysosomal pathway, apoptosis, and fibrosis all contribute to the rapid development of total cataracts.

BetaB2-crystallin is a predominant structural protein and plays a key role in the development and maintenance of lens transparency.[33] To date, more than 40 mutations in its coding gene *Crybb2* have been reported to be associated with congenital cataract.[34] A previous study demonstrated that mutations in βB2-crystallin cause protein structure abnormalities, resulting in unstable proteins that precipitate from solution and cataract formation.[6] In our previous study, we identified a missense mutation in exon 6 of *Crybb2* that led to an exchange of Trp for Cys (W151C) in four generations of a Chinese family affected with congenital membranous cataracts. We also found that the mutation damaged the solubility of βB2-crystallin and resulted in the formation of aggregates in cells.[7] In βB2-W151C knock-in mice, we found that the development of lens opacity was obviously accelerated at 2 to 3 months of age and advanced to total cataracts at 3 months of age. In addition, fibrosis of the lens capsule and epithelium occurred in the lenses of W151C +/+ mice at 3 months of age. Therefore, the decrease in protein solubility induced by the mutation cannot explain all the pathological changes in the lens, such as LEC EMT and the sudden acceleration of cataract development.

In this study, whole genome transcriptomics analysis revealed that ERS and ERS-induced apoptosis and the stagnation of protein synthesis play major roles in the rapid development of W151C mutant-induced congenital cataract. The results of real-time PCR and Western blot further validated that ERS was activated in the progression of lens opacity. A previous study suggested that Perk/Eif2α pathway was activated and ERS was induced in mouse congenital nuclear cataract caused by the connexin50D47A mutation. The trigger of ERS increases *Chop* expression and results in lens cell apoptosis.[13] In addition, in *Col4a1*

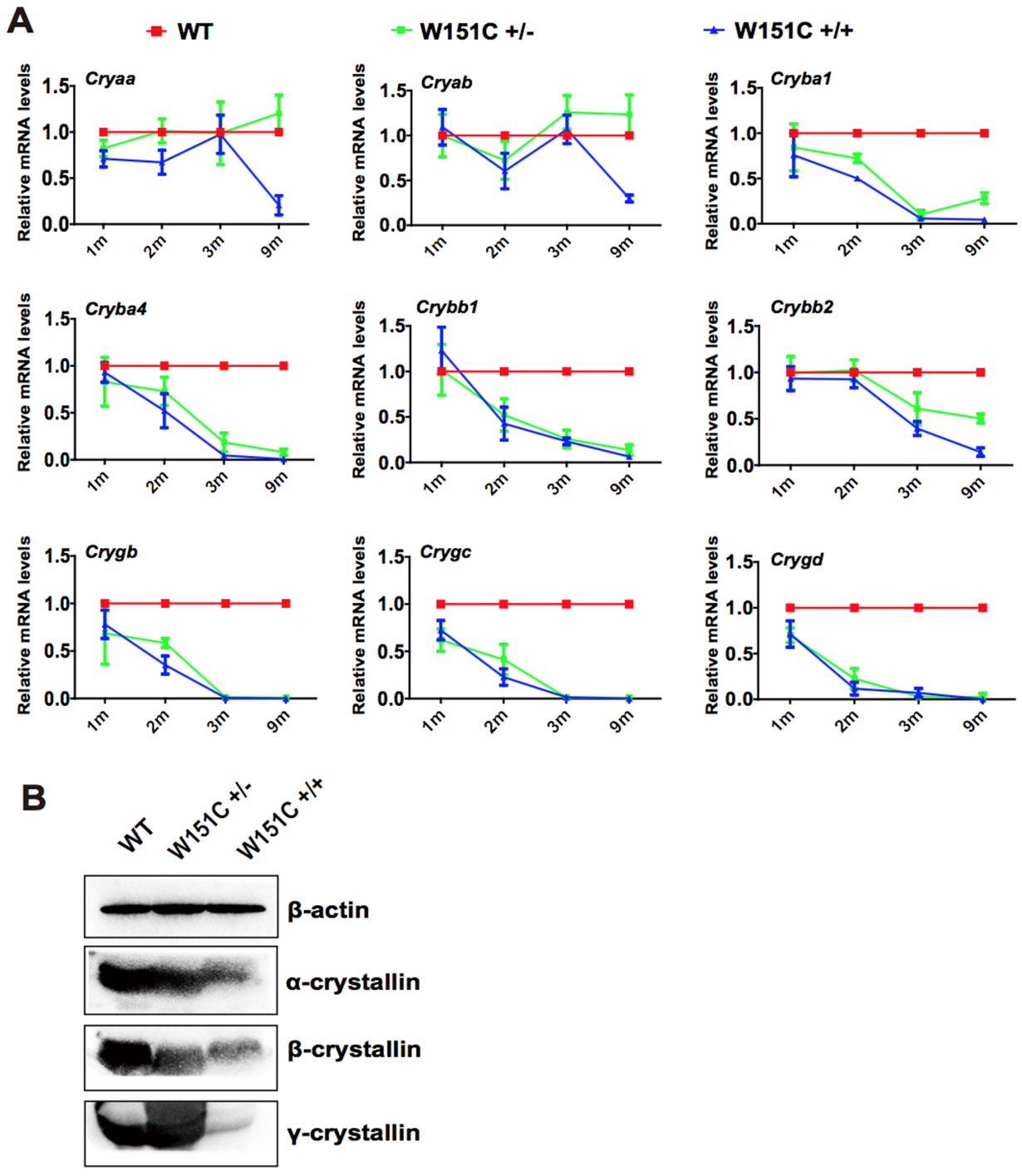

Figure 5. ERS-mediated stagnation of crystallin synthesis plays a critical role during the accelerated development of congenital cataract. (**A**) Real-time PCR analysis of the expression of crystalline-coding genes such as *Cryaa*, *Cryab*, *Cryba1*, *Cryba4*, *Crybb1*, *Crybb2*, *Crygb*, *Crygc*, and *Crygd* in the lenses of WT, W151C +/−, and W151C +/+ mice at 3, 6, and 9 months of age. The experiments were repeated independently three or more times. (**B**) Western blot analysis of α-, β-, and γ-crystallin protein levels in the lenses of WT, W151C +/-, and W151C +/+ mice at 3 months of age. The experiments were repeated independently three or more times.

transgenic and mutant mouse cataract models, abnormal accumulation of collagen IV activated the Irel/Xbp1, Atf6, and Perk pathways to activate the UPR, and the activation of the UPR reduced the synthesis of β and γ-crystallin proteins, thus disrupting the differentiation of lens fibers and resulting in cell apoptosis, eventually leading to the formation of cataract.[17] Our study also demonstrated that the transcription and the translation of various proteins in the lens were dramatically reduced during the rapid progression of cataracts. This may contribute to the disarray and degeneration of lens fiber cells in the later stage of cataract development. Another interesting point in our results is that the maintenance of the expression of αA and αB-crystallins until late in the process. We think these results are consistent with their roles as molecular chaperones.

Investigative Ophthalmology & Visual Science

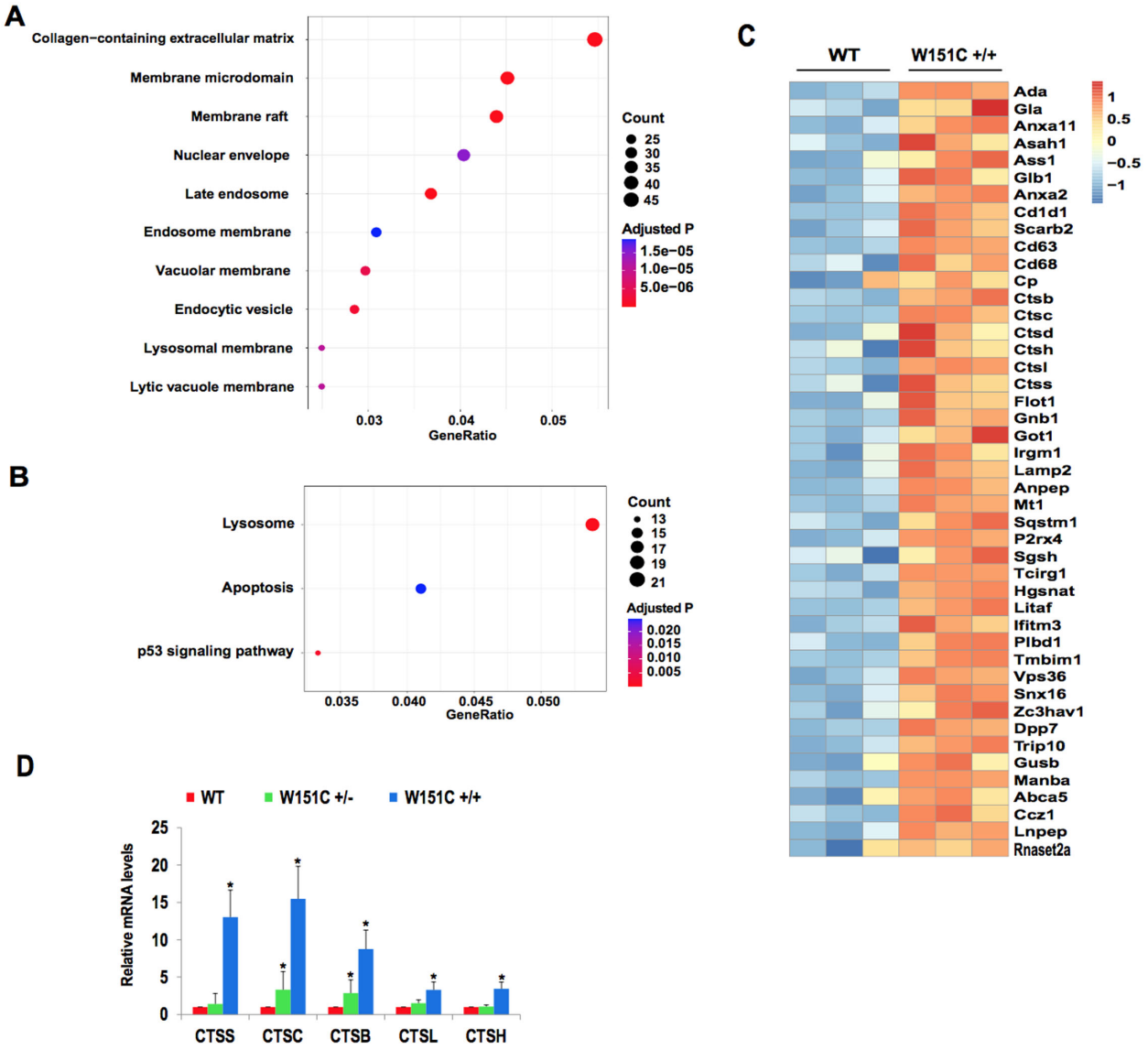

Figure 6. The lysosomal pathway is also involved in the rapid progression of congenital cataract induced by the βB2-W151C mutant. (**A**) Dotplot visualizing the top 10 Gene Ontology (GO) biological processes in homozygous lenses at 3 months of age. The size of the dots represents the number of associated genes (count). (**B**) Dotplot visualizing the pathways of DEGs enrichment, as determined by KEGG analysis. The size of the dots represents the number of associated genes (count). GeneRatio = (count of upregulated genes in each GO term or KEGG pathway)/(count of total upregulated genes). (**C**) Heatmap showing that lysosome-related genes were dramatically upregulated in the lenses of homozygous mice at 3 months of age. (**D**) Real-time PCR analysis was used to validate the transcript levels of cathepsins in the lenses of 3-month-old W151C +/-, W151C +/+, and WT mice. *, $P < 0.05$ versus WT control mice. The experiments were repeated independently three or more times.

Moreover, the results of transcriptional profiling of the lens in W151C mutant mice revealed that lysosomes and lysosomal proteases, especially cathepsins were distinctly upregulated during the progression of W151C mutant-induced congenital cataracts. Cysteine cathepsins, including cathepsins B, C, F, H, K, L, O, S, V, W, and X, are the most important proteases in lysosomes. Previous studies have reported that cathepsins are released and then process Bid and degrade the antiapoptotic protein Bcl-2, thereby triggering apoptosis through engagement of the mitochondrial pathway.[18] However, the functions of these proteins in the lens have not yet been established. In the current study, transcriptional profiling showed that apoptotic signaling pathways were activated in the lenses of W151C mice. Therefore, we suggested that lens cell apoptosis induced by ERS and the lysosomal pathway is an important mechanism that accelerates the development of cataracts.

LEC EMT and lens capsule fibrosis have not been reported in congenital cataract. In the current study, the histology results showed that lenses developed multilayered LEC plaques beneath the anterior capsule at 3 months of age and progressed to severe whole capsule fibrosis at 9 months of age. Whole genome transcriptomics analysis also revealed that more than 20 fibrosis-related genes were significantly upregulated in homozygous mice. Previous studies have demonstrated that ERS is an important regulator of EMT in many tissues.[35–38] ERS induction and UPR can promote

Investigative Ophthalmology & Visual Science

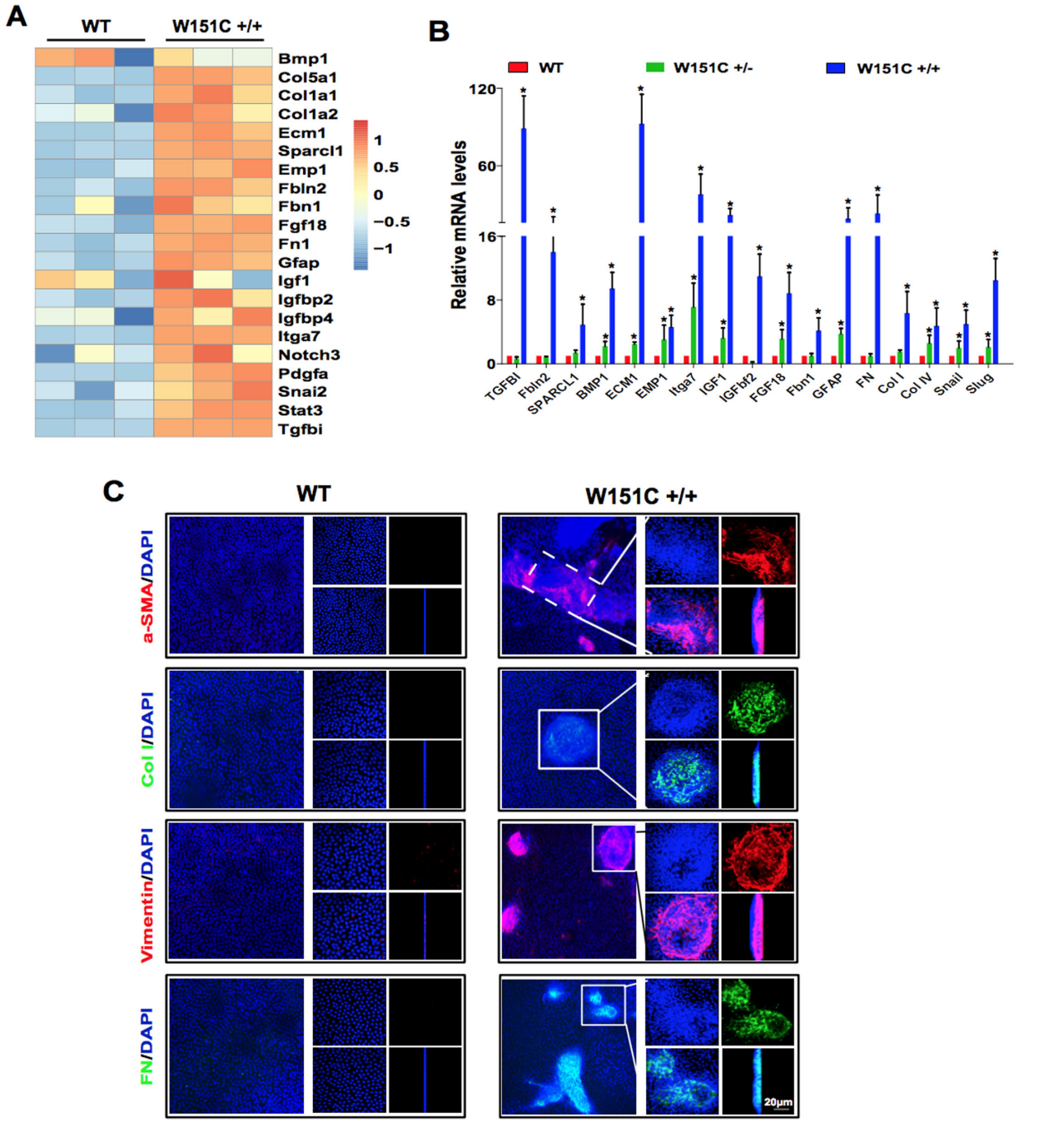

Figure 7. LEC EMT and lens capsule fibrosis contribute to lens cortex liquefaction in the late stage of congenital cataract. (**A**) Heatmap showing that EMT-related genes were dramatically upregulated in the lenses of W151C +/+ mice at 3 months of age. (**B**) Real-time PCR analysis was used to validate the transcript levels of EMT-related genes in the lens of W151C +/−, W151C +/+, and WT mice at 3 months of age. *, $P < 0.05$ versus WT control mice. The experiments were repeated independently three or more times. (**C**) Immunofluorescent staining analysis of the EMT markers α-SMA, Col I, Vimentin, and FN in the lens capsule whole-mounts of W151C +/+ and WT mice ($n = 6$ eyes per group). Representative confocal microscopy 3D images of lens capsule whole-mounts are shown.

EMT through the Smad, Perk, Mapk, β-catenin, and Src signaling pathways in endometrial and pulmonary fibrosis.[37,39,40] Therefore, we speculated that lens fibrosis was induced by the activation of ERS in W151C mutant mice. Due to fibrosis of the lens capsule, its barrier function was damaged, and permeability was changed, resulting in gradual hydrolysis of the lens cortex at the late stage of congenital cataract.

In summary, the W151C mutation in βB2-crystallin causes progressive bilateral congenital cataracts. In addition to a decrease in protein solubility, ERS and ERS-mediated stagnation of lens protein synthesis, the lysosomal pathway, apoptosis, and fibrosis contribute to the accelerated development of cataracts. These results indicated the inhibition of ERS and lysosomal cathepsins may be promising therapeutic strategies for congenital cataract.

Investigative Ophthalmology & Visual Science

Acknowledgments

Supported by the Guangdong Basic and Applied Basic Research Foundation (2023A1515030108 and 2023A1515012192).

Disclosure: **W. Xiao**, None; **W. Yang**, None; **X. Zhang**, None; **X. Deng**, None; **X. Chen**, None

References

1. Hejtmancik JF. Congenital cataracts and their molecular genetics. *Semin Cell Dev Biol.* 2008;19(2):134–149.
2. Lampi KJ, Ma Z, Shih M, et al. Sequence analysis of betaA3, betaB3, and betaA4 crystallins completes the identification of the major proteins in young human lens. *J Biol Chem.* 1997;272(4):2268–2275.
3. Feng J, Smith DL, Smith JB. Human lens beta-crystallin solubility. *J Biol Chem.* 2000;275(16):11585–11590.
4. Fu L, Liang JJ. Detection of protein-protein interactions among lens crystallins in a mammalian two-hybrid system assay. *J Biol Chem.* 2002;277(6):4255–4260.
5. Liu BF, Liang JJ. Interaction and biophysical properties of human lens Q155* betaB2-crystallin mutant. *Mol Vis.* 2005;11:321–327.
6. Reddy MA, Bateman OA, Chakarova C, et al. Characterization of the G91del CRYBA1/3-crystallin protein: A cause of human inherited cataract. *Hum Mol Genet.* 2004;13(9):945–953.
7. Chen W, Chen X, Hu Z, et al. A missense mutation in CRYBB2 leads to progressive congenital membranous cataract by impacting the solubility and function of betaB2-crystallin. *PLoS One.* 2013;8(11):e81290.
8. Haeri M, Knox BE. Endoplasmic reticulum stress and unfolded protein response pathways: Potential for treating age-related retinal degeneration. *J Ophthalmic Vis Res.* 2012;7(1):45–59.
9. Chan P, Stolz J, Kohl S, Chiang WC, Lin JH. Endoplasmic reticulum stress in human photoreceptor diseases. *Brain Res.* 2016;1648(Pt B):538–541.
10. Zode GS, Kuehn MH, Nishimura DY, et al. Reduction of ER stress via a chemical chaperone prevents disease phenotypes in a mouse model of primary open angle glaucoma. *J Clin Invest.* 2011;121(9):3542–3553.
11. Gow A, Sharma R. The unfolded protein response in protein aggregating diseases. *Neuromolecular Med.* 2003;4(1-2):73–94.
12. Hetz C. The unfolded protein response: Controlling cell fate decisions under ER stress and beyond. *Nat Rev Mol Cell Biol.* 2012;13(2):89–102.
13. Berthoud VM, Minogue PJ, Lambert PA, Snabb JI, Beyer EC. The cataract-linked mutant connexin50D47A causes endoplasmic reticulum stress in mouse lenses. *J Biol Chem.* 2016;291(34):17569–17578.
14. Alapure BV, Stull JK, Firtina Z, Duncan MK. The unfolded protein response is activated in connexin 50 mutant mouse lenses. *Exp Eye Res.* 2012;102:28–37.
15. Ma Z, Yao W, Chan CC, Kannabiran C, Wawrousek E, Hejtmancik JF. Human betaA3/A1-crystallin splicing mutation causes cataracts by activating the unfolded protein response and inducing apoptosis in differentiating lens fiber cells. *Biochim Biophys Acta.* 2016;1862(6):1214–1227.
16. Andley UP, Goldman JW. Autophagy and UPR in alpha-crystallin mutant knock-in mouse models of hereditary cataracts. *Biochim Biophys Acta.* 2016;1860(1 Pt B):234–239.
17. Firtina Z, Danysh BP, Bai X, Gould DB, Kobayashi T, Duncan MK. Abnormal expression of collagen IV in lens activates unfolded protein response resulting in cataract. *J Biol Chem.* 2009;284(51):35872–35884.
18. Repnik U, Stoka V, Turk V, Turk B. Lysosomes and lysosomal cathepsins in cell death. *Biochim Biophys Acta.* 2012;1824(1):22–33.
19. Satoh K, Takemura Y, Satoh M, Ozaki K, Kubota S. Loss of FYCO1 leads to cataract formation. *Sci Rep.* 2021;11(1):13771.
20. Wignes JA, Goldman JW, Weihl CC, Bartley MG, Andley UP. p62 expression and autophagy in alpha B-crystallin R120G mutant knock-in mouse model of hereditary cataract. *Exp Eye Res.* 2013;115:263–273.
21. Chen JH, Huang C, Zhang B, et al. Mutations of RagA GTPase in mTORC1 pathway are associated with autosomal dominant cataracts. *PLoS Genet.* 2016;12(6):e1006090.
22. Tu C, Li H, Liu X, et al. TDRD7 participates in lens development and spermiogenesis by mediating autophagosome maturation. *Autophagy.* 2021;17(11):3848–3864.
23. Hegde S, Kesterson RA, Srivastava OP. CRYbetaA3/A1-crystallin knockout develops nuclear cataract and causes impaired lysosomal cargo clearance and calpain activation. *PLoS One.* 2016;11(2):e0149027.
24. Sagona AP, Nezis IP, Stenmark H. Association of CHMP4B and autophagy with micronuclei: Implications for cataract formation. *Biomed Res Int.* 2014;2014:974393.
25. Chen X, Xiao W, Chen W, et al. MicroRNA-26a and -26b inhibit lens fibrosis and cataract by negatively regulating Jagged-1/Notch signaling pathway. *Cell Death Differ.* 2017;24(11):1990.
26. Ritchie ME, Phipson B, Wu D, et al. Limma powers differential expression analyses for RNA-sequencing and microarray studies. *Nucleic Acids Res.* 2015;43(7):e47.
27. Wu T, Hu E, Xu S, et al. ClusterProfiler 4.0: A universal enrichment tool for interpreting omics data. *Innovation (Camb).* 2021;2(3):100141.
28. Bustin SA, Benes V, Garson JA, et al. The MIQE guidelines: Minimum information for publication of quantitative real-time PCR experiments. *Clin Chem.* 2009;55(4):611–622.
29. Mungrue IN, Pagnon J, Kohannim O, Gargalovic PS, Lusis AJ. CHAC1/MGC4504 is a novel proapoptotic component of the unfolded protein response, downstream of the ATF4-ATF3-CHOP cascade. *J Immunol.* 2009;182(1):466–476.
30. Choi J, Park SY, Joo CK. Transforming growth factor-beta1 represses E-cadherin production via slug expression in lens epithelial cells. *Invest Ophthalmol Vis Sci.* 2007;48(6):2708–2718.
31. Liu Z, Lin H, Jin G, et al. In-the-bag versus ciliary sulcus secondary intraocular lens implantation for pediatric aphakia: A prospective comparative study. *Am J Ophthalmol.* 2022;236:183–192.
32. Zhao WJ, Xu J, Chen XJ, Liu HH, Yao K, Yan YB. Effects of cataract-causing mutations W59C and W151C on betaB2-crystallin structure, stability and folding. *Int J Biol Macromol.* 2017;103:764–770.
33. Andley UP. Crystallins in the eye: Function and pathology. *Prog Retin Eye Res.* 2007;26(1):78–98.
34. Shiels A, Bennett TM, Hejtmancik JF. Cat-Map: Putting cataract on the map. *Mol Vis.* 2010;16:2007–2015.
35. Zhou S, Yang J, Wang M, Zheng D, Liu Y. Endoplasmic reticulum stress regulates epithelial–mesenchymal transition in human lens epithelial cells. *Mol Med Rep.* 2020;21(1):173–180.
36. Tong B, Fu L, Hu B, et al. Tauroursodeoxycholic acid alleviates pulmonary endoplasmic reticulum stress and epithelial-mesenchymal transition in bleomycin-induced lung fibrosis. *BMC Pulm Med.* 2021;21(1):149.
37. Meng X, Liu K, Xie H, et al. Endoplasmic reticulum stress promotes epithelial–mesenchymal transition via the PERK signaling pathway in paraquat–induced pulmonary fibrosis. *Mol Med Rep.* 2021;24(1)525.

Investigative Ophthalmology & Visual Science

38. Yoon S, Shin B, Woo HG. Endoplasmic reticulum stress induces CAP2 expression promoting epithelial-mesenchymal transition in liver cancer cells. *Mol Cells*. 2021;44(8):569–579.
39. Bao M, Feng Q, Zou L, Huang J, Zhu C, Xia W. Endoplasmic reticulum stress promotes endometrial fibrosis through the TGF-beta/SMAD pathway. *Reproduction*. 2023;165(2):171–182.
40. Tanjore H, Cheng DS, Degryse AL, et al. Alveolar epithelial cells undergo epithelial-to-mesenchymal transition in response to endoplasmic reticulum stress. *J Biol Chem*. 2011;286(35):30972–30980.

Investigative Ophthalmology & Visual Science